

1
2
3
4
5
6
7
8
9
10
11
12
13
14
15
16
17
18
19
20
21
22
23
24
25
26
27

MISS DIANA MICATI (Orcid ID : 0000-0003-3503-9434)

Article type : Original Article

Differential expression profiles of conserved Snail transcription factors in the mouse testis

Diana J Micati^{1,7}, Gary R Hime², Eileen A McLaughlin^{3,4}, *Helen E Abud⁵, and *Kate L Loveland^{1,6,7}

*Helen E Abud and Kate L Loveland are senior co-authors

1. Department of Molecular and Translational Sciences, Monash University, Melbourne, Victoria, 3800, Australia
2. Department of Anatomy and Neuroscience, University of Melbourne, Melbourne, Australia
3. School of Environmental and Life Sciences, University of Newcastle, Callaghan, NSW, 2308, Australia
4. School of Biological Sciences, University of Auckland, Auckland, 1152, New Zealand
5. Cancer Program, Monash Biomedicine Discovery Institute and Department of Anatomy and Developmental Biology, Monash University, Victoria, 3800, Australia
6. Department of Anatomy and Developmental Biology, Monash University, Melbourne, Victoria, 3800, Australia
7. Centre for Reproductive Health, Hudson Institute of Medical Research, Melbourne, Victoria, 3168, Australia

Correspondence should be addressed to K.L.

Phone +61 3 8572 2904

This is the author manuscript accepted for publication and has undergone full peer review but has not been through the copyediting, typesetting, pagination and proofreading process, which may lead to differences between this version and the [Version of Record](#). Please cite this article as [doi: 10.1111/andr.12465](https://doi.org/10.1111/andr.12465)

This article is protected by copyright. All rights reserved

28 Address: Level 3, MHRP Building, Hudson Institute of Medical Research, 27-31 Wright
29 Street, Clayton, 3168, Australia

30 Email: kate.loveland@monash.edu

31 Running title: Snail expression in mammalian testis

32 **Funding information:** Work was supported by grants from the National Health and Medical
33 Research Council of Australia (Project grant ID1048110 to GH, HA, KL and Fellowship
34 ID1079646 to KL).

35

36

37 **Abstract**

38

39 Snail transcription factors are key regulators of cellular transitions during embryonic
40 development and tumorigenesis. The closely related SNAI1 and SNAI2 proteins induce
41 epithelial-mesenchymal transitions (EMTs), acting predominantly as transcriptional
42 repressors, while the functions of SNAI3 are unknown. An initial examination of *Snai2*-
43 deficient mice provided evidence of deficient spermatogenesis. To address the hypothesis that
44 Snail proteins are important for male fertility, this study provides the first comprehensive
45 cellular expression profiles of all three mammalian Snail genes in the postnatal mouse testis.
46 To evaluate Snail transcript expression profiles, droplet digital (dd) PCR and *in situ*
47 hybridisation were employed. *Snai1*, 2, and 3 transcripts are readily detected at 7, 14, 28 days
48 postpartum (dpp) and 7 weeks (adult). Unique cellular expression was demonstrated for each
49 by *in situ* hybridisation and immunohistochemistry using Western blot-validated antibodies.
50 SNAI1 and SNAI2 are in the nucleus of the most mature germ cell types at postnatal ages 10,
51 15, and 26. SNAI3 is only detected from 15 dpp onwards, and is localised in the Sertoli cell
52 cytoplasm. In the adult testis, *Snai1* and *Snai2* transcripts are detected in spermatogonia and
53 spermatocytes, while *Snai3* is in both germ and Sertoli cells. SNAI1 protein is evident in
54 nuclei of spermatogonia, spermatocytes, round spermatids, and elongated spermatids (Stages
55 IX-XII). SNAI2 is present in the nuclei of spermatogonia and spermatocytes, with a faint
56 signal detected in round spermatids. SNAI3 was detected only in Sertoli cell cytoplasm, as in
57 the juvenile testes. Additionally, co-localisation of SNAI1 and SNAI2 with previously

58 identified key binding partners, LSD1 and PRC2 complex components, provides strong
59 evidence that these important functional interactions are conserved during spermatogenesis to
60 control gene activity. These distinct expression profiles suggest that each Snail family
61 member has unique functions during spermatogenesis.

62

63

64 **Keywords**

65 Snail transcription factors – Postnatal mouse testis - Germ cells – Spermatogenesis - Cycle of
66 the seminiferous epithelium

67

68 **Introduction**

69 Spermatogenesis is characterized by a series of essential cellular transitions that are required
70 for the production of functional spermatozoa. Each spermatogenic stage involves changes in
71 gene expression that are tightly regulated, and this study addresses the hypothesis that Snail
72 transcription factors contribute to the correct progression of germline development.

73 Snail proteins belong to a large superfamily of zinc-finger transcription factors that play
74 crucial roles in transcriptional regulation, cellular migration, chromatin remodelling, cell
75 signalling and impact on many developmental processes (Batlle, Sancho et al. 2000, Kalluri
76 and Weinberg 2009, Lin, Dong et al. 2014), including mesoderm formation and neural crest
77 cell migration during embryogenesis (Alberga, Boulay et al. 1991). Additionally, Snail
78 family members are overexpressed in various cancers where they are major regulators of cell
79 survival, proliferation, and invasion (Turner, Broad et al. 2006, Uygur and Wu 2011).

80 The mammalian Snail family has three members, SNAI1, SNAI2, and SNAI3. Each features
81 a highly conserved carboxy- (C) terminal region and a more divergent amino (N) terminal
82 region, particularly for SNAI3 (Kataoka, Murayama et al. 2000, Nieto 2002). A conserved
83 DNA-binding domain within the C-terminus contains four to six zinc fingers which directly
84 interact with target genes to regulate their activity. The N-terminal region is composed of the
85 SNAG transactivation domain, which interacts both directly and indirectly with co-factor
86 proteins to form multi-molecular structures that drive target gene repression (Chiang and
87 Ayyanathan 2013). Snail co-factors are chromatin remodelling enzymes. These include:

88 LSD1, HDAC1/2, EZH2, G9a and SUV39H1 (Lin, Dong et al. 2014), and several of these
89 have critical roles in the reprogramming of the transcriptome during spermatogenesis,
90 promoting both spermatogonial differentiation (Myrick, Christopher et al. 2017), and
91 progression of meiosis (Mu, Starmer et al. 2014).

92 Spermatogenesis is a complex process by which mature spermatozoa are produced through a
93 series of cellular divisions and maturation steps, each featuring a unique transcriptome
94 (Ahmed and de Rooij 2009, Shalet 2009). Germ cells are strictly organised within the
95 seminiferous epithelium formed by Sertoli cells, so that each generation of spermatogonia,
96 spermatocytes and spermatids develops in parallel with subsequent generations, in a highly
97 ordered, cyclic manner, termed Stages (Leblond and Clermont 1952). The cycle of the
98 seminiferous epithelium of the adult mouse testis is considered as divided into 12 Stages (I-
99 XII) (Oakberg 1956, Hess and Renato de Franca 2008). In mice, the first complete cycle of
100 spermatogenesis commences at 7 days post-partum (dpp) and yields spermatozoa by 42 dpp. .
101 Key time points corresponding to the first appearance of a particular germ cell type have been
102 identified during the first wave of spermatogenesis. At 7 dpp, the mouse seminiferous cords
103 contain only Sertoli cells and spermatogonia. At 14 dpp, spermatocytes are present within the
104 tubules which form when post-mitotic Sertoli cells secrete fluids in an apical directions. As a
105 result of meiotic divisions, round spermatids are first formed at 28 dpp. These haploid cells
106 undergo morphological changes to first produce elongated spermatids at 30 dpp, and
107 functional spermatozoa by 35 dpp (Fig. 1 a) (Kramer and Erickson 1981). The transition from
108 one spermatogenic cell type to the next is governed by tight control of transcription (Eddy
109 1998). This progressive emergence of each more mature germ cell type during the first wave
110 of spermatogenesis in juveniles provides a good opportunity to visualise how the dynamic
111 changes in gene expression are coordinated by transcriptional regulators.

112 The *Snai*-deficient mice for which a testicular phenotype has been reported are those lacking
113 *Snai2* which exhibit pigmentation, epithelial and hematopoietic defects (Cobaleda, Perez-
114 Caro et al. 2007). The testis was only analysed in these *Snai2* deficient mice at six week of
115 age; they display testicular atrophy, resulting from an apparent reduction in germ cell number
116 (Perez-Losada, Sanchez-Martin et al. 2002), although this has not been quantitated. In
117 addition, *Snai2* knockout mice are reported to be subfertile. Fertility was analysed in other
118 *Snai*-deficient mouse models. Specifically, the complete absence of *Snai3* does not affect the
119 testicular phenotype (Bradley, Norton et al. 2013), implying that SNAI3 is not necessary for
120 spermatogenesis. However mice lacking both *Snai2* and *Snai3* have been reported to be

121 infertile (Pioli, Dahlem et al. 2013), suggesting that SNAI2 and SNAI3 are functionally
122 redundant in the testis. This result is surprising given the structural differences between
123 SNAI2 and SNAI3; this potential has not been investigated further. A different study,
124 examining ubiquitin ligase β -TrCP knockout mice, provided indirect evidence that elevated
125 SNAI1 levels can impair spermatogenesis. In this strain, the prominent nuclear SNAI1
126 immunostaining in spermatogonia suggested that SNAI1 was not targeted for proteasomal
127 degradation and resulted in spermatogonial cell loss (Kanarek, Horwitz et al. 2010).
128 However, analysis of the testes in both of these mouse models was limited. In the present
129 study, ddPCR, *in situ* hybridisation and immunohistochemistry are used to document the
130 cellular expression profiles of all three Snail family members in the normal postnatal mouse
131 testis, including during pre- and post-pubertal development. The findings reveal distinct
132 cellular expression profiles for the Snail mRNAs and proteins that are concordant with
133 developmental switches during cellular differentiation. Importantly, we provide evidence that
134 these co-localise with previously identified Snail co-factors, thereby providing a platform for
135 understanding the potential functions of Snail family members during the cellular transitions
136 of spermatogenesis.

137

138 **Materials and Methods**

139 **Animal Ethics**

140 All procedures involving animal samples were approved by the Monash Animal Research
141 Platform (MARF) Ethics Committee and conformed to the National Health and Medical
142 Research Council (NHMRC) of Australia's Code of Practice for the Care and Use of Animals
143 for Experimental Purposes.

144

145 **Mouse tissues and histological sections**

146 For histology, C57Bl/6J mice were obtained from (MARF). Testis sections at various ages
147 including 10, 15, 26 days post-partum (dpp) and adult (60-90 dpp) were first fixed in Bouin's
148 or 4% PFA for 3-5 hrs, then paraffin-embedded using the Shandon Histocentre 3 (Thermo
149 Electron Corporation) at the Monash University Histology Facility. Sections of 5 μ m were
150 dried onto Superfrost 2 glass slides (Menzel-Glaser, Braunschweig, Germany). *Snai2*
151 knockout tissue was obtained from the *Snai2*^{LacZ} mouse line, generated by replacing the zinc

152 finger coding region of the *Snai2* gene with the β -galactosidase gene (Jiang, Lan et al. 1998).
153 PFA-fixed adult mouse testis samples (*Snai2*^{+/+}, n=1; and *Snai2*^{-/-}, n=1) were kindly
154 provided by Professor Donna Frances Kusewitt (MD Anderson, Smithville, Texas) to verify
155 the specificity of the SNAI2 antibody.

156

157 *Droplet digital PCR*

158 Total RNA was extracted from four decapsulated Swiss mouse testes at postnatal days 7, 14,
159 28 and adult (Week 7) using TRIzol reagent (Invitrogen, Thermo Fisher Scientific, Waltham,
160 USA). Genomic DNA contamination was eliminated by DNase treatment using DNase-free
161 kit (Ambion, Thermo Fisher Scientific, Waltham, USA). cDNA was synthesised using 100 U
162 Superscript III reverse transcriptase (Invitrogen, Thermo Fisher Scientific, Waltham, USA)
163 with 2.5 μ M random hexamer oligonucleotides (Roche, Basal, Switzerland). Methods were
164 performed according to manufacturers' instructions. cDNA was diluted 1:10 with filtered
165 MilliQ water and quantified using the QIAxpert system (QIAGEN, Hilden, Germany).

166 The cDNAs from enriched preparations of spermatogonia (> 95% pure; n = 3),
167 spermatocytes (> 85% pure; n = 3) and round spermatids (> 88% pure; n = 2) were used in
168 previous studies and supplied at a 1:10 dilution for these experiments. Spermatogonia had
169 been isolated from 8 days old mouse testes, while 8 week old mouse testes were used for
170 isolation of spermatocytes and round spermatids. Samples were collected from a 2-4%
171 continuous bovine serum albumin (BSA) gradient, as previously described (McIver, Stanger
172 et al. 2012, Bromfield, Aitken et al. 2017).

173 Digital droplet (dd) PCR was performed using the BioRad QX100/200 system. The ddPCR
174 reaction contained 12.5 μ l of 2 x ddPCR Supermix for probes (BioRad, Hercules, USA),
175 1.25 μ l of 20 x target probes with a FAM dye label (final concentration 250 nM each), 2 μ l of
176 1:10 template dilution, and filtered MilliQ water to a final volume of 25 μ l. Twenty μ l of
177 ddPCR reaction followed by 70 μ l of droplet generator oil for probes (BioRad, Hercules,
178 USA) were loaded into a DG8TM cartridge for the QX100/200 droplet generator (BioRad,
179 Hercules, USA). Droplets produced were transferred into a 96 well plate (Eppendorf,
180 Hamburg, Germany) and a two-step thermocycling protocol [(enzyme activation at 95°C x 10
181 mins); 40 cycles x (denaturation at 94°C x 30s, annealing at 59°C x 60s, enzyme deactivation
182 at 98°C X 10 mins), ramp rate set at 2.5°C/s] was performed in a thermalcycler (BioRad
183 C1000 Touch). The plate was then placed in a QX100/200 Droplet Reader (BioRad,

184 Hercules, USA). Data were analysed using the QuantaSoft analysis software (BioRad,
185 Hercules, USA). Age series values and isolated germ cell data were not normalised. Data
186 were reported as the means \pm standard error of the means (SEM).

187 Probes, supplied by IDT (Coralville, USA), were: *Snai1* (MmPT. 58.43057042); *Snai2*
188 (MmPT. 58.5576027); *Snai3* (MmPT. 58.43894205).

189

190 *DIG-labelled RNA probes and in situ hybridisation*

191 Primer sequences used to generate *in situ* hybridisation probes are listed in Table 1. The
192 following PCR parameters were used to amplify target transcript regions: 95°C for 3 mins; 40
193 cycles of 95°C (30s), 61°C (30s), 72°C (30s); 72°C for 7 mins using 1 μ l cDNA. Templates
194 used were adult mouse testis (to amplify *Snai1* and *Snai3*) and 6 dpp (to amplify *Snai2*). PCR
195 products were purified (QIAquick PCR Purification Kit, QIAGEN, Hilden, Germany), cloned
196 in pGEM T-Easy vector (Promega, Madison, USA) following the manufacturer's guidelines
197 and sequenced (Big Dye Terminator v3.1 Cycle Sequencing Kit, ABIPRISM 377 DNA
198 Sequencer, Applied Biosystems) by the Gandel Charitable Trust Sequencing Centre, Hudson
199 Institute of Medical Research, Clayton, VIC, Australia. PCR amplification of these plasmids
200 using pBS forward and reverse primers produced products that included T7 and Sp6
201 polymerase binding sites which were used as templates for *in vitro* transcription to generate
202 antisense and sense cRNA probes (Itman, Wong et al. 2011).

203 *In situ* hybridisation was performed on Bouin's fixed, paraffin embedded, adult mouse testis
204 sections to determine the cellular sites where *Snai1*, *Snai2* and *Snai3* transcripts are
205 synthesised using standard procedures (Itman, Wong et al. 2011). Briefly, slides were
206 dewaxed and rehydrated. To permeabilise the tissue, sections were incubated with Proteinase
207 K solution (Roche, Basal, Switzerland) at 37°C for 30 mins. Tissue sections were incubated
208 with Prehybridisation buffer (50% v/v DIF, 14% v/v 20 x SSC, 33% v/v phosphate buffer,
209 4% v/v 50 x Denhardt's solution) for 2 hrs at 50 - 55°C in a hybridisation oven within a
210 covered humid chamber. Hybridisation was performed with 150 ng/100 μ l probe per slide at
211 50 - 55°C overnight, followed by washes of 15 mins from 2 x SSC to 0.1 x SSC at the
212 hybridisation temperature. Bound DIG-labelled cRNA probes were detected by anti-DIG
213 antibody (1:1000 dilution, Roche, Basal, Switzerland) and visualised by alkaline phosphatase
214 developer (BCIP/NBT, Thermo Fisher Scientific, Waltham, USA). Slides were
215 counterstained with Harris Hematoxylin (diluted 1:3 v/v) and mounted under coverslips in

216 GVA aqueous solution (Genemed Biotechnologies, South San Francisco, USA). In situ
217 hybridisation was performed three times using adult testis sections from two different mice.
218 Slides were imaged on a Zeiss imager A.1 microscope with an AxioCam MRc5.

219

220 *Immunohistochemistry*

221 Immunohistochemistry was performed as previously described (Dias, Rajpert-De Meyts et al.
222 2009). Immunostaining with anti-SNAI1, anti-SNAI2, anti-EED, anti-EZH2, and anti-LSD1
223 was performed on PFA-fixed testis sections, whereas SNAI3 immunostaining was performed
224 on Bouin's fixed testis sections. Slides were dewaxed and rehydrated. Antigen retrieval was
225 performed by heating slides for 10 mins in 10 mM citrate buffer (pH 6.0) using a 1000 W
226 Pressure Cooker (Tefal). Slides were then treated with 0.3% hydrogen peroxide for 5 min at
227 RT and washed 2 x 5 min at RT in tris-buffered saline (50 mM Tris, 150 mM NaCl, pH 7.5)
228 (TBS). Blocking solution and antibody diluent consisted of 5% (v/v) normal serum diluted in
229 TBS/0.1% BSA [(Sigma Aldrich, St Louis, USA) (to detect SNAI3)] or CAS block
230 [(Invitrogen, Thermo Fisher Scientific, Waltham, USA) (to detect SNAI1 and SNAI2)] added
231 for 1 hr at RT in a humid chamber. Sections were incubated overnight with primary antibody
232 at RT in a humid chamber. Antibodies used to detect SNAI1 (GeneTex, GTX125918; 1:100),
233 SNAI2 (abcam, ab27568, 1:100), SNAI3 (Santa Cruz Biotechnology, sc10439, 1:100), EED
234 (R&D system, #AF5827, 1:200), EZH2 (Cell Signaling Technology, #5246, 1:200), LSD1
235 (abcam, ab17721, 1:200). Anti-SNAI1, anti-SNAI2, anti-EZH2, and anti-LSD1 were detected
236 using biotinylated anti-rabbit secondary antibody (Invitrogen, #656140, 1:500). SNAI3 was
237 detected using biotinylated anti-goat secondary antibody (DAKO, #E0466, 1:500), whereas
238 biotinylated anti-sheep secondary antibody was used for EED (Thermo Scientific, #618640,
239 1:500). Signal was amplified with Vectastain Elite ABC kit reagents according to the
240 manufacturer's instructions (Vector Laboratories, Burlingame, USA) followed by detection
241 with DAB (3,3-diaminobenzidine tetrahydrochloride, DAKO, Steinheim, USA) to produce a
242 brown precipitate. Sections were counterstained with Harris hematoxylin (Sigma Aldrich, St
243 Louis, USA), dehydrated and mounted using DPX (Sigma Aldrich, St Louis, USA). Control
244 sections were incubated in the absence of primary antibody to check for non-specific
245 reactivity. Slides were imaged on a Zeiss imager A.1 microscope with an AxioCam MRc5.

246 The EED antibody used in this study was validated on *Eed* knockout samples (Prokopuk,
247 Stringer et al. 2017). The specificity of EZH2 antibody is evident over 75 publications,

248 including the chromatin immunoprecipitation (ChIP) application (Snitow, Li et al. 2015). The
249 specificity of LSD1 antibody is evident over 99 publications, including the ChIP application
250 (Muralidharan, Khatri et al. 2017). The SNAI1 antibody was previously validated on *Snai1*
251 knockout tissue (Horvay, Jarde et al. 2015). Western blots were performed in this study to
252 validate the SNAI1, SNAI2 and SNAI3 antibodies using mouse testis lysates (see
253 Supplementary Materials and Methods). The specificity of the SNAI2 antibody was further
254 validated on *Snai2* knockout testis samples.

255

256 **Results**

257 **Snail mRNAs are expressed in distinct cell populations during postnatal testis** 258 **development**

259 To determine the pattern of Snail mRNA and protein expression through mouse testis
260 development, we performed ddPCR and immunohistochemistry, respectively. *Snai1*, *Snai2*
261 and *Snai3* transcripts were measured by ddPCR using RNA extracted from postnatal ages 7,
262 14, 28 and adult (week 7) whole mouse testes. These ages correspond to germ cell population
263 shifts that occur during the first postnatal wave of male germ cell development (Fig. 1 a). At
264 day 7, the only cells present in the seminiferous tubule are undifferentiated and differentiated
265 spermatogonia, and immature Sertoli cells. At day 14, spermatogonia and early
266 spermatocytes are present, Sertoli cell proliferation has just arrested and tight junctions have
267 begun to form between adjacent Sertoli cells to create the epithelial barrier required to
268 support post-mitotic spermatogenesis. At day 28, spermatogonia, spermatocytes, round
269 spermatids, and mature Sertoli cells are present. In the adult testis, all germ cell subtypes are
270 present, including elongated spermatids, in addition to mature Sertoli cells. Droplet digital
271 (dd) PCR revealed that all Snail family member genes were expressed at every postnatal age
272 examined in the testis (Fig. 1 b-d). The *Snai1* transcript was detected at similar levels at each
273 age (Fig. 1 b), suggesting that *Snai1* mRNA is present in multiple cell types within the testis.
274 The *Snai2* transcript was most abundant at day 7, then significantly declined and was
275 consistent through to adulthood (Fig. 1 c). The *Snai3* transcript was present at relatively low
276 and consistent levels in all ages, but most abundant at day 7 (Fig. 1 d). This implies that
277 *Snai2* and *Snai3* transcripts are enriched within the cells present prior the transition of mitotic
278 to meiotic cells.

279

280 **Snail transcription factors display distinct mRNA profiles in the adult mouse testis and**
281 **in isolated germ cells**

282 We next conducted a detailed analysis of Snail transcription factors in the adult mouse testis.
283 This delineated the specific germ cell types in which Snail mRNAs are expressed, as the
284 progression of germ cells between each differentiation state to form mature spermatozoa can
285 be readily observed. To determine the cellular expression profiles of Snail transcripts, *in situ*
286 hybridisation was performed on fixed wild-type adult mouse testis sections. *Snai1* was
287 predominantly detected in spermatogonia and spermatocytes, with a faint signal apparent in
288 round spermatids (Fig. 2 a, d). Similarly, the *Snai2* signal was strong in spermatogonia and
289 spermatocytes, but not detectable in haploid germ cells (Fig. 2 b, e). *Snai3* showed a less
290 restricted expression profile, with a signal evident in the cytoplasm of all germ cells and
291 Sertoli cells (Fig. 2 c, f). *In situ* hybridisation results were verified by ddPCR which provided
292 measurements of Snail transcript levels in isolated germ cells. Consistent with the *in situ*
293 hybridisation data, *Snai1* and *Snai2* levels were higher in spermatogonia (Fig. 2 g) and
294 spermatocytes (Fig. 2 j), but drastically lower in round spermatids (Fig. 2 k). In comparison,
295 *Snai3* levels were highest in spermatogonia (Fig. 2 g), but significantly lower in
296 spermatocytes and round spermatids (Fig. 2 j, k).

297

298 **Snail transcription factors display unique protein expression profiles during postnatal**
299 **testis development**

300 To gain further understanding of the potential function of Snail transcription factors, we
301 analysed Snail protein localisation in the postnatal mouse testis during the first wave of
302 spermatogenesis. Germ and Sertoli cells were identified by their size, shape and chromatin
303 morphology. SNAI1 displayed nuclear immunostaining in spermatogonia at day 10 (Fig. 3 a),
304 in spermatogonia and spermatocytes at day 15 (Fig. 3 b) and in spermatogonia, spermatocytes
305 and round spermatids at day 26 (Fig. 3 c). At postnatal days 10 and 15, SNAI2 was detected
306 in the nucleus of spermatogonia, but was in the cytoplasm of spermatocytes at day 15 (Fig 3
307 e). At day 26, SNAI2 was localised in the nucleus of spermatogonia, spermatocytes, round
308 and elongated spermatids (Fig. 3 g), but in the adult mouse testis, SNAI2 appeared to be
309 restricted in the nucleus of spermatogonia and spermatocytes, with a faint signal only in
310 round spermatids (Fig. 3 h, Fig. S1). These data suggest that SNAI1 and SNAI2 are active
311 during major cellular transitions. During the first wave of spermatogenesis, SNAI3

312 immunostaining was not detectable at day 10 (Fig. 3 i). A signal restricted to the Sertoli cell
313 cytoplasm was observed at postnatal ages 15 (Fig. 3 j), 26 (Fig. 3 k), and in the adult (Fig. 3 l,
314 Fig S2). However, the SNAI3 protein profile was different to that of its transcript, detected by
315 *in situ* hybridisation in both germ and Sertoli cells in the adult mouse testis (Fig. 2 c, f). This
316 suggests that there is tight regulation of SNAI3 transcript and protein synthesis.

317 Western blots were performed using lysates from adult mouse testis, isolated germ cells and
318 whole mouse embryo (e11.5) to assess antibody specificity (Fig. S3). A single band at ~ 24
319 kDa for SNAI1 was detected in 30 µg lysates from whole adult mouse testis and isolated
320 germ cells. Additionally, two bands of expected sizes for SNAI3 were observed at ~ 45 and
321 ~47 kDa in 30 µg lysates from whole embryo at e11.5 and adult mouse testis. SNAI2 could
322 not be readily detected by Western blot. To determine specificity of antibody,
323 immunohistochemistry was performed on adult testis from a *Snai2* knockout mouse (Fig. S3
324 d). Compared to control, SNAI2 was absent from spermatogonia and spermatocytes. Non-
325 specific signal was detected in the cytoplasm of elongated spermatids.

326 Overall these results demonstrate that the expression pattern of Snail transcription factors is
327 dynamic, suggesting that each Snail family member has a unique role in the developing
328 mouse testis.

329

330 **SNAI1 subcellular localisation in the adult mouse testis is Stage-specific**

331 Snail transcription factors are required to be nuclear in order to function. We investigated the
332 subcellular localisation of SNAI1 in adult mouse testis by immunohistochemistry using an
333 antibody that was previously used for detecting nuclear SNAI1 in intestinal cells (Horvay,
334 Jarde et al. 2015). Interestingly, SNAI1 appeared to be nuclear in germ cells at specific
335 Stages of the seminiferous epithelium cycle. At Stages I-VIII, strong signal was seen in the
336 nucleus of spermatogonia, pachytene spermatocytes, and round spermatids (Fig. 4 a-c). At
337 Stages IX-XII, some spermatogonia, pachytene and meiotically dividing spermatocytes
338 displayed an intense nuclear staining; signal was absent from leptotene and zygotene
339 spermatocytes (Fig. 4 d, e). The localisation of SNAI1 in elongated spermatids is particularly
340 intriguing, as it changed. At Stages IX-XII, SNAI1 was in the nucleus of elongating
341 spermatids (Fig. 4 d, e, g-j), but the signal became cytoplasmic at Stages I-VII (Fig. 4 a-c).
342 This indicates that SNAI1 may have a specific role during the period of global transcriptional
343 repression in elongating spermatids that occurs at Stages IX-XII.

344

345 **SNAI1 and SNAI2 share protein localisation patterns with co-repressors in the adult**
346 **mouse testis.**

347 Snail family members need to recruit co-factors to mediate transcriptional repression. To
348 understand the mechanism of Snail-mediated transcriptional regulation, we investigated the
349 expression of EED and EZH2, PRC2 complex components, and LSD1 in the adult mouse
350 testis, each of which is known to co-operate functionally with SNAI1 and SNAI2 (Mu,
351 Starmer et al. 2014, Myrick, Christopher et al. 2017). By immunohistochemistry, EED and
352 EZH2 displayed nuclear localisation in spermatogonia, leptotene, zygotenes, pachytene and
353 meiotically dividing spermatocytes, and in Sertoli cells at Stages I-XII (Fig. 5). These
354 proteins were detected in round spermatid nuclei at Stages I-VI (Fig. 5 a, b, f, g), while these
355 signals were restricted to the cytoplasm of round spermatids at Stage VII-VIII (Fig. 5 c, h).

356 LSD1, lysine-specific histone demethylase 1, showed subcellular localisation profiles
357 identical to SNAI1 in the adult mouse testis, with nuclear signal in spermatogonia,
358 spermatocytes, round spermatids and Sertoli cells (Fig. 6). Like SNAI1, nuclear LSD1 was
359 observed in elongated spermatids in a Stage-specific manner. At Stages IX-XII, LSD1 was
360 nuclear in elongating spermatids (Fig. 6 d, e), but restricted to the cytoplasm of elongated
361 spermatids following nuclear condensation at Stages I-VII (Fig. 6 a-c). Overall, these results
362 identify potential partners required for Snail-mediated transcriptional regulation during
363 spermatogenesis.

364

365 **Discussion**

366 Snail factors are of central importance to transcriptional regulation, cellular migration, signal
367 transduction and chromatin remodelling in many developmental and disease systems, but
368 their functional relevance to male fertility are poorly understood. As an initial approach to
369 addressing this knowledge gap, we identified the cellular production sites of Snail
370 transcription factors in the postnatal mouse testis. We show here for the first time that each
371 Snail family members' transcript and protein has a distinct, developmentally regulated
372 expression profile in cells of the postnatal mouse testis. This strongly suggests that each Snail
373 family member has a distinct function during spermatogenesis.

374 SNAI1, SNAI2 and SNAI3 have similar molecular structures, however there are differences
375 in their biological actions. SNAI1 functions as a potent survival factor (Vega, Morales et al.
376 2004) and is essential to the preservation of stem cell function (Miller and Gauthier-Fisher
377 2009) (Horvay, Jarde et al. 2015). Gene repression is best understood to be its mechanism of
378 mediating these outcomes (De Craene, van Roy et al. 2005). In the testis, SNAI1 was
379 previously suggested to be associated with spermatogonial stem cell maintenance; indirect
380 upregulation of SNAI1 resulted in disruption of adherens junctions within the seminiferous
381 epithelium and loss of spermatogonia (Kanarek, Horwitz et al. 2010). The present study
382 describing SNAI1 mRNA and protein expression in the postnatal and adult mammalian testis
383 provides new information that highlights the potential for SNAI1 to function at specific
384 stages of spermatogenesis. Analyses by ddPCR and immunohistochemistry show that SNAI1
385 mRNA and protein are present at every age in the postnatal testis (Fig. 1, Fig. 3).
386 Intriguingly, SNAI1 protein is present in the nucleus of the most mature germ cell type
387 present at each age, suggesting that SNAI1 is involved in the regulation of developmental
388 switches during the cellular transitions of spermatogenesis. This function associated with
389 SNAI1 is well-described during the epithelial to mesenchymal transition (EMT), in which
390 nuclear-localised SNAI1 drives epithelial cells to acquire mesenchymal characteristics via the
391 reprogramming of gene expression; key outcomes are cytoskeletal reorganisation and
392 changes in cell behaviour (Wang, Shi et al. 2013). In the adult mouse testis (Fig. 2, Fig. 4), *in*
393 *situ* hybridisation and ddPCR identify *Snail* predominantly in spermatocytes, although a less
394 intense signal is also detected in spermatogonia and round spermatids. At a post-translational
395 level, our analysis reveals a Stage- and cell-specific profile for SNAI1 protein in the adult
396 mouse testis. SNAI1 is confined to the nucleus of a restricted number of spermatogonia, and
397 of pachytene and diplotene spermatocytes, suggesting it could regulate gene transcription in
398 both mitotic and meiotic germ cells. The two domains of Snail that are required for
399 interaction with downstream targets and for recruitment of co-factors may be central to
400 determining its diverse functions during spermatogenesis. In the post-meiotic phase, SNAI1
401 localises within spermatid nuclei at Stages VIII-XII (Fig. 4), during the interval of extensive
402 morphological changes that includes chromatin reorganisation and compaction. In the
403 nucleus, histones are gradually replaced first by histone variants and transition proteins
404 (Stages VIII-XII), then finally by protamines (Stages I-VII). As DNA is packaged,
405 transcription is down-regulated (Hermo, Pelletier et al. 2010). Major contributors to
406 transcriptional repression in spermatids are chromatin remodelling enzymes, capable of
407 methylating or demethylating histones at specific residues (Rathke, Baarends et al. 2014).

408 Histone lysine demethylases 1 (LSD1) mediates transcriptional repression via demethylation
409 of H3K4 (Gu and Lee 2013), and in the adult mouse testis LSD1 is observed in spermatid
410 nuclei at Stages VIII-XII (Fig. 6). Consistent with the capacity of SNAI1 to recruit chromatin
411 remodelling complexes at the SNAG domain, our results suggest that SNAI1 may interact
412 with LSD1 to potentially mediate DNA packaging and promote repression of gene
413 transcription.

414 Like SNAI1, SNAI2 regulates transcription and mediates the EMT (Villarejo, Cortes-Cabrera
415 et al. 2014), however each induces common and distinct gene expression outcomes, as shown
416 in epithelial cells (Moreno-Bueno, Cubillo et al. 2006). Specific SNAI2 functions in the testis
417 are unknown, although it appears to be important for male fertility. Histological sections from
418 *Snai2*-deficient mice were interpreted as displaying reduced germ and somatic Leydig cell
419 numbers in the testis, though this outcome was not further quantified. This was hypothesised
420 to arise from the disruption of the stem cell factor (SCF)/KIT signalling pathway, of known
421 critical importance to spermatogonial cell migration, proliferation and differentiation. Droplet
422 digital PCR indicates that the SNAI2 transcript and protein are present throughout postnatal
423 testis development (Fig. 1, Fig. 3). In the adult testis, *in situ* hybridisation and ddPCR
424 identified *Snai2* as more highly expressed in spermatocytes than in spermatogonia (Fig. 2).
425 Consistent with the mRNA data, SNAI2 protein was detected in the nucleus of
426 spermatogonia, and spermatocytes with a faint signal also observed in spermatids, thus
427 SNAI2 may be involved in the events relating to mitotic and meiotic germ cell progression.
428 Interestingly, EZH2 and EED, components of the PRC2 complex, co-localise with SNAI2 in
429 nuclei of spermatogonia, spermatocytes and round spermatids (Fig. 5). Known for its unique
430 roles in maintaining the undifferentiated spermatogonial pool through regulating SSC self-
431 renewal, and in progression of meiosis (Mu, Starmer et al. 2014), the PRC2 complex
432 represents a strong candidate to initiate SNAI2-mediate transcriptional repression. Because
433 PRC2 controls many targets, it is not surprising that its spermatogenic phenotype, featuring
434 the absence of post-meiotic cells, is more severe than that of *Snai2* knockout.

435

436 SNAI1 and SNAI2 are known to compensate for each other's loss by binding to the same
437 target gene regulatory sequences (Chen and Gridley 2013). In the postnatal testis, we
438 demonstrated that both SNAI1 and SNAI2 localise in the nucleus of spermatogonia and
439 spermatocytes, where they may be functionally redundant. However SNAI3 displayed a

440 distinct expression profile. SNAI3 is structurally divergent and only recruits target genes with
441 specific E-box sequences to its zinc finger domain. SNAI3 represses gene activity via its
442 SNAG domain and an additional non-zinc finger region (Kataoka, Murayama et al. 2000).
443 Although *Snai3* transcript is highly expressed in the skeletal muscle and thymus of adult
444 wildtype mice (Kataoka, Murayama et al. 2000), its function is unknown. In this study, we
445 demonstrate that *Snai3* is present at low levels at every age in the postnatal mouse testis (Fig.
446 1), indicating that it is restricted to a selected population of cells. In the adult mouse testis, *in*
447 *situ* hybridisation reveals that *Snai3* is expressed in Sertoli and all germ cells (Fig. 2). The
448 *Snai3* expression profile in germ cells was confirmed by ddPCR, with *Snai3* levels higher in
449 spermatogonia and spermatocytes, but lower in round spermatids (Fig. 2). In the developing
450 postnatal testis, SNAI3 protein was visible in the Sertoli cell cytoplasm from 15 dpp, but not
451 earlier, until adulthood (Fig. 3), indicating that SNAI3 might have a specific role during the
452 formation of Sertoli-germ cell adherens junctions, Sertoli-Sertoli tight junctions, which
453 contribute to the blood-testis barrier. It is intriguing that the major components of the
454 adherens and tight junctions are E-Cadherin (Tanwar, Zhang et al. 2011), occludins and
455 claudins, essential for blood-testis barrier integrity (Morrow, Mruk et al. 2010) and well-
456 known Snail downstream targets (Nieto 2002, Ikenouchi, Matsuda et al. 2003). The absence
457 of a SNAI3 protein signal in any germ cells may reflect a high turnover or lack of synthesis in
458 the spermatogenic lineage. To our knowledge, there is no evidence for alternative isoforms.

459

460 In summary, this study has provided evidence that synthesis of each of the three mammalian
461 Snail transcription factor is tightly regulated during mouse spermatogenesis. The cellular
462 distribution of Snail transcripts and proteins in the postnatal mouse testis indicates their likely
463 sites of function, including in relationship to the regulatory mechanisms that mediate
464 developmental changes during cellular transitions in spermatogenesis and during Sertoli cell
465 development. These data provide a foundation for defining what regulates Snail levels and
466 target genes, many of which are implicated in key processes in other biological systems.

467

468 **Acknowledgments:** The authors would like to thank Reyhan Akhtar, Dr Katja Horvay and
469 Franca Casagrande for assistance with Droplet digital PCR. The authors acknowledge
470 Elizabeth Richards and Penny Whiley for technical support. We also like to thank Dr Patrick

471 Western and Dr Jody Haigh for providing aliquots of the EED and EZH2, and LSD1
472 antibodies, respectively.

473 **Author Contributions:** DJM, KLL, HEA, GRH designed experiments, interpreted data and
474 wrote the manuscript. DJM performed experiments. EAM provided materials for the study.

475 **Compliance with ethical standards**

476 **Conflict of interest:** The authors have no conflicts of interest in presenting information and
477 material described in this paper.

478

479

480 **References**

481 Ahmed, E. A. and D. G. de Rooij (2009). "Staging of mouse seminiferous tubule cross-sections."
482 *Methods Mol Biol* **558**: 263-277.

483

484 Alberga, A., J. L. Boulay, E. Kempe, C. Dennefeld and M. Haenlin (1991). "The snail gene required for
485 mesoderm formation in *Drosophila* is expressed dynamically in derivatives of all three germ layers."
486 *Development* **111**(4): 983-992.

487

488 Batlle, E., E. Sancho, C. Franci, D. Dominguez, M. Monfar, J. Baulida and A. Garcia De Herreros
489 (2000). "The transcription factor snail is a repressor of E-cadherin gene expression in epithelial
490 tumour cells." *Nat Cell Biol* **2**(2): 84-89.

491

492 Bradley, C. K., C. R. Norton, Y. Chen, X. Han, C. J. Booth, J. K. Yoon, L. T. Krebs and T. Gridley (2013).
493 "The snail family gene *snai3* is not essential for embryogenesis in mice." *PLoS One* **8**(6): e65344.

494

495 Bromfield, E. G., R. J. Aitken, E. A. McLaughlin and B. Nixon (2017). "Proteolytic degradation of heat
496 shock protein A2 occurs in response to oxidative stress in male germ cells of the mouse." *Mol Hum
497 Reprod* **23**(2): 91-105.

498

499 Chen, Y. and T. Gridley (2013). "Compensatory regulation of the *Snai1* and *Snai2* genes during
500 chondrogenesis." *J Bone Miner Res* **28**(6): 1412-1421.

501

502 Chiang, C. and K. Ayyanathan (2013). "Snail/Gfi-1 (SNAG) family zinc finger proteins in transcription
503 regulation, chromatin dynamics, cell signaling, development, and disease." *Cytokine Growth Factor*
504 *Rev* **24**(2): 123-131.

505

506 Cobaleda, C., M. Perez-Caro, C. Vicente-Duenas and I. Sanchez-Garcia (2007). "Function of the zinc-
507 finger transcription factor SNAI2 in cancer and development." *Annu Rev Genet* **41**: 41-61.

508

509 De Craene, B., F. van Roy and G. Berx (2005). "Unraveling signalling cascades for the Snail family of
510 transcription factors." *Cell Signal* **17**(5): 535-547.

511

512 Dias, V. L., E. Rajpert-De Meyts, R. McLachlan and K. L. Loveland (2009). "Analysis of activin/TGFB-
513 signaling modulators within the normal and dysfunctional adult human testis reveals evidence of
514 altered signaling capacity in a subset of seminomas." *Reproduction* **138**(5): 801-811.

515

516 Eddy, E. M. (1998). "Regulation of gene expression during spermatogenesis." *Semin Cell Dev Biol*
517 **9**(4): 451-457.

518

519 Gu, B. and M. G. Lee (2013). "Histone H3 lysine 4 methyltransferases and demethylases in self-
520 renewal and differentiation of stem cells." *Cell Biosci* **3**(1): 39.

521

522 Hermo, L., R. M. Pelletier, D. G. Cyr and C. E. Smith (2010). "Surfing the wave, cycle, life history, and
523 genes/proteins expressed by testicular germ cells. Part 2: changes in spermatid organelles associated
524 with development of spermatozoa." *Microsc Res Tech* **73**(4): 279-319.

525

526 Hess, R. A. and L. Renato de Franca (2008). "Spermatogenesis and cycle of the seminiferous
527 epithelium." *Adv Exp Med Biol* **636**: 1-15.

528 Horvay, K., T. Jarde, F. Casagrande, V. M. Perreau, K. Haigh, C. M. Nefzger, R. Akhtar, T. Gridley, G.
529 Berx, J. J. Haigh, N. Barker, J. M. Polo, G. R. Hime and H. E. Abud (2015). "Snai1 regulates cell lineage
530 allocation and stem cell maintenance in the mouse intestinal epithelium." *EMBO J* **34**(10): 1319-
531 1335.

532

533 Ikenouchi, J., M. Matsuda, M. Furuse and S. Tsukita (2003). "Regulation of tight junctions during the
534 epithelium-mesenchyme transition: direct repression of the gene expression of claudins/occludin by
535 Snail." *J Cell Sci* **116**(Pt 10): 1959-1967.

536

537 Itman, C., C. Wong, P. A. Whiley, D. Fernando and K. L. Loveland (2011). "TGFbeta superfamily
538 signaling regulators are differentially expressed in the developing and adult mouse testis."
539 *Spermatogenesis* **1**(1): 63-72.

540

541 Jiang, R., Y. Lan, C. R. Norton, J. P. Sundberg and T. Gridley (1998). "The Slug gene is not essential for
542 mesoderm or neural crest development in mice." *Dev Biol* **198**(2): 277-285.

543

544 Kalluri, R. and R. A. Weinberg (2009). "The basics of epithelial-mesenchymal transition." *J Clin Invest*
545 **119**(6): 1420-1428.

546

547 Kanarek, N., E. Horwitz, I. Mayan, M. Leshets, G. Cojocaru, M. Davis, B. Z. Tsuberi, E. Pikarsky, M.
548 Pagano and Y. Ben-Neriah (2010). "Spermatogenesis rescue in a mouse deficient for the ubiquitin
549 ligase SCF{beta}-TrCP by single substrate depletion." *Genes Dev* **24**(5): 470-477.

550

551 Kataoka, H., T. Murayama, M. Yokode, S. Mori, H. Sano, H. Ozaki, Y. Yokota, S. Nishikawa and T. Kita
552 (2000). "A novel snail-related transcription factor Smuc regulates basic helix-loop-helix transcription
553 factor activities via specific E-box motifs." *Nucleic Acids Res* **28**(2): 626-633.

554

555 Kramer, J. M. and R. P. Erickson (1981). "Developmental program of PGK-1 and PGK-2 isozymes in
556 spermatogenic cells of the mouse: specific activities and rates of synthesis." *Dev Biol* **87**(1): 37-45.

557

558 Leblond, C. P. and Y. Clermont (1952). "Definition of the stages of the cycle of the seminiferous
559 epithelium in the rat." *Ann N Y Acad Sci* **55**(4): 548-573.

560

561 Lin, Y., C. Dong and B. P. Zhou (2014). "Epigenetic regulation of EMT: the Snail story." *Curr Pharm*
562 *Des* **20**(11): 1698-1705.

563

564 McIver, S. C., S. J. Stanger, D. M. Santarelli, S. D. Roman, B. Nixon and E. A. McLaughlin (2012). "A
565 unique combination of male germ cell miRNAs coordinates gonocyte differentiation." *PLoS One* **7**(4):
566 e35553.

567

568 Miller, F. D. and A. Gauthier-Fisher (2009). "Home at last: neural stem cell niches defined." *Cell Stem*
569 *Cell* **4**(6): 507-510.

570

571 Moreno-Bueno, G., E. Cubillo, D. Sarrio, H. Peinado, S. M. Rodriguez-Pinilla, S. Villa, V. Bolos, M.
572 Jorda, A. Fabra, F. Portillo, J. Palacios and A. Cano (2006). "Genetic profiling of epithelial cells
573 expressing E-cadherin repressors reveals a distinct role for Snail, Slug, and E47 factors in epithelial-
574 mesenchymal transition." *Cancer Res* **66**(19): 9543-9556.

575

576 Morrow, C. M., D. Mruk, C. Y. Cheng and R. A. Hess (2010). "Claudin and occludin expression and
577 function in the seminiferous epithelium." *Philos Trans R Soc Lond B Biol Sci* **365**(1546): 1679-1696.

578

579 Mu, W., J. Starmer, A. M. Fedoriw, D. Yee and T. Magnuson (2014). "Repression of the soma-specific
580 transcriptome by Polycomb-repressive complex 2 promotes male germ cell development." *Genes
581 Dev* **28**(18): 2056-2069.

582

583 Muralidharan, B., Z. Khatri, U. Maheshwari, R. Gupta, B. Roy, S. J. Pradhan, K. Karmodiya, H.
584 Padmanabhan, A. S. Shetty, C. Balaji, U. Kolthur-Seetharam, J. D. Macklis, S. Galande and S. Tole
585 (2017). "LHX2 Interacts with the NuRD Complex and Regulates Cortical Neuron Subtype
586 Determinants Fezf2 and Sox11." *J Neurosci* **37**(1): 194-203.

587

588 Myrick, D. A., M. A. Christopher, A. M. Scott, A. K. Simon, P. G. Donlin-Asp, W. G. Kelly and D. J. Katz
589 (2017). "KDM1A/LSD1 regulates the differentiation and maintenance of spermatogonia in mice."
590 *PLoS One* **12**(5): e0177473.

591

592 Nieto, M. A. (2002). "The snail superfamily of zinc-finger transcription factors." *Nat Rev Mol Cell Biol*
593 **3**(3): 155-166.

594

595 Oakberg, E. F. (1956). "Duration of spermatogenesis in the mouse and timing of stages of the cycle of
596 the seminiferous epithelium." *Am J Anat* **99**(3): 507-516.

597

598 Perez-Losada, J., M. Sanchez-Martin, A. Rodriguez-Garcia, M. L. Sanchez, A. Orfao, T. Flores and I.
599 Sanchez-Garcia (2002). "Zinc-finger transcription factor Slug contributes to the function of the stem
600 cell factor c-kit signaling pathway." *Blood* **100**(4): 1274-1286.

601

602 Pioli, P. D., T. J. Dahlem, J. J. Weis and J. H. Weis (2013). "Deletion of Snai2 and Snai3 results in
603 impaired physical development compounded by lymphocyte deficiency." *PLoS One* **8**(7): e69216.

604

605 Prokopuk, L., J. M. Stringer, K. Hogg, K. D. Elgass and P. S. Western (2017). "PRC2 is required for
606 extensive reorganization of H3K27me3 during epigenetic reprogramming in mouse fetal germ cells."
607 *Epigenetics Chromatin* **10**: 7.

608

609 Rathke, C., W. M. Baarends, S. Awe and R. Renkawitz-Pohl (2014). "Chromatin dynamics during
610 spermiogenesis." *Biochim Biophys Acta* **1839**(3): 155-168.

611

612 Shalet, S. M. (2009). "Normal testicular function and spermatogenesis." *Pediatr Blood Cancer* **53**(2):
613 285-288.

614

615 Snitow, M. E., S. Li, M. P. Morley, K. Rathi, M. M. Lu, R. S. Kadzik, K. M. Stewart and E. E. Morrisey
616 (2015). "Ezh2 represses the basal cell lineage during lung endoderm development." *Development*
617 **142**(1): 108-117.

618

619 Tanwar, P. S., L. Zhang and J. M. Teixeira (2011). "Adenomatous polyposis coli (APC) is essential for
620 maintaining the integrity of the seminiferous epithelium." *Mol Endocrinol* **25**(10): 1725-1739.

621

622 Turner, F. E., S. Broad, F. L. Khanim, A. Jeanes, S. Talma, S. Hughes, C. Tselepis and N. A. Hotchin
623 (2006). "Slug regulates integrin expression and cell proliferation in human epidermal keratinocytes."
624 *J Biol Chem* **281**(30): 21321-21331.

625

626 Uygur, B. and W. S. Wu (2011). "SLUG promotes prostate cancer cell migration and invasion via
627 CXCR4/CXCL12 axis." *Mol Cancer* **10**: 139.

628

629 Vega, S., A. V. Morales, O. H. Ocana, F. Valdes, I. Fabregat and M. A. Nieto (2004). "Snail blocks the
630 cell cycle and confers resistance to cell death." *Genes Dev* **18**(10): 1131-1143.

631

632 Villarejo, A., A. Cortes-Cabrera, P. Molina-Ortiz, F. Portillo and A. Cano (2014). "Differential role of
633 Snail1 and Snail2 zinc fingers in E-cadherin repression and epithelial to mesenchymal transition." *J*
634 *Biol Chem* **289**(2): 930-941.

635

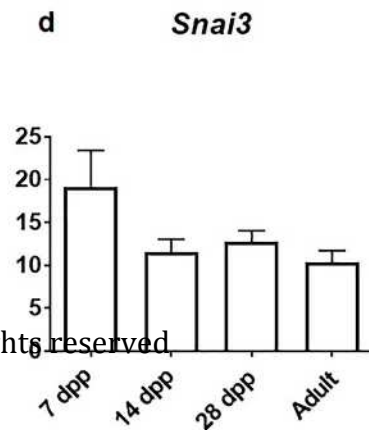
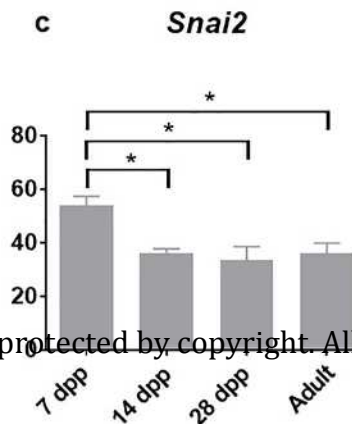
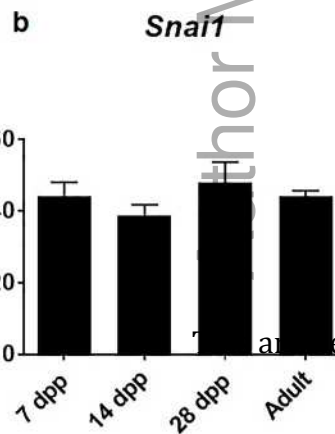
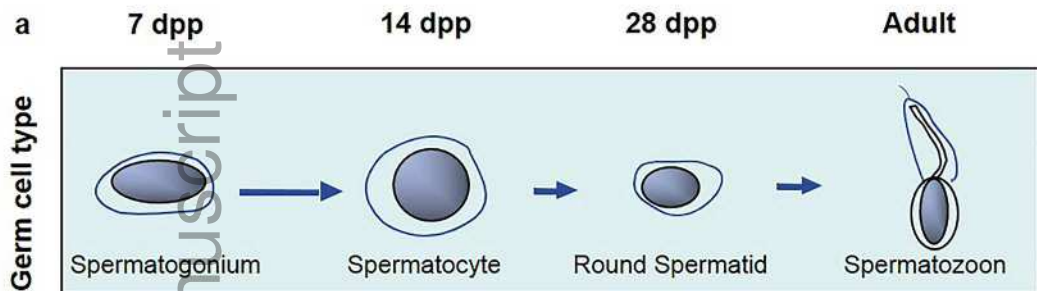
636 Wang, Y., J. Shi, K. Chai, X. Ying and B. P. Zhou (2013). "The Role of Snail in EMT and Tumorigenesis."
637 *Curr Cancer Drug Targets* **13**(9): 963-972.

Author Manuscript

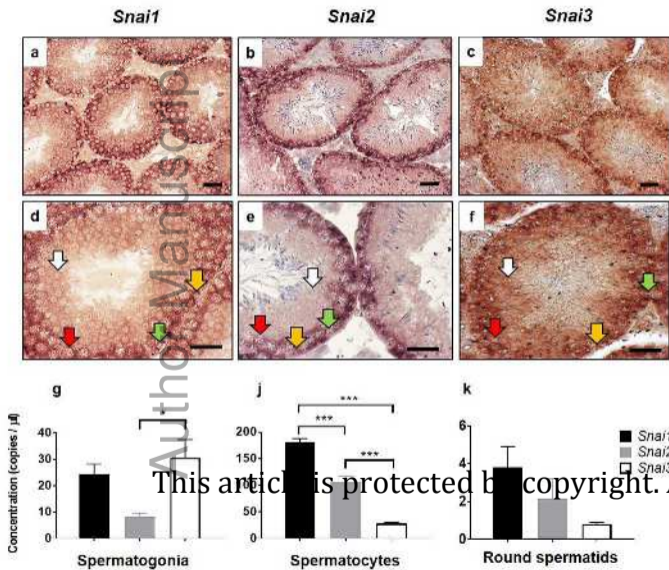
Gene	Accession number	Forward (5'-3')	Reverse (5'-3')	Region amplified
Snai1	NM_011427.3	TTCAGGCCACCTTCTTTGAG	TGAAACAGGTGTCACCAGGA	1178-1353
Snai2	NM_011415.2	TGATGCCTGGTTGTCATCAG	GACACGCACCAGGAATGTTT	1462-1666
Snai3	NM_013914.2	TCTGCTGGACCTGTTCCAAA	GGGGCAGGAGAAAATGTGTC	1159- 1373

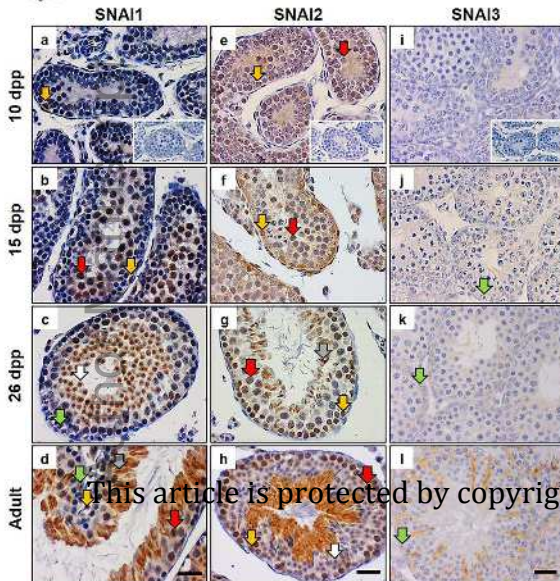
Table 1. Primer sequences used for generation of in situ hybridisation probes to detect mouse transcripts.

Fig. 1

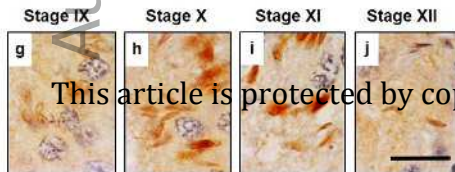
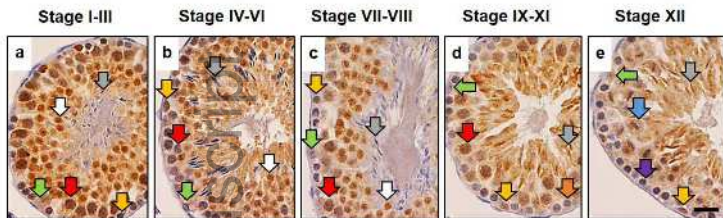


bioRxiv preprint doi: <https://doi.org/10.1101/124651>; this version posted July 11, 2017. The copyright holder for this preprint (which was not certified by peer review) is the author/funder, who has granted bioRxiv a license to display the preprint in perpetuity. It is made available under aCC-BY-NC-ND 4.0 International license.



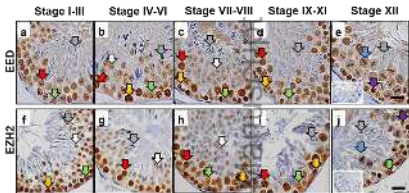


This article is protected by copyright. All rights reserved.



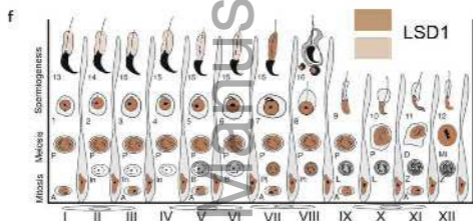
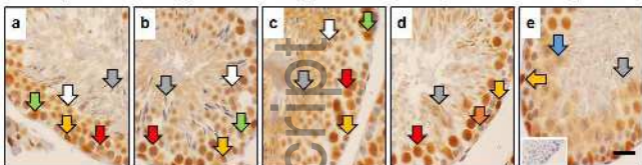
This article is protected by copyright. All rights reserved.

andr_12465_f5.pdf



This article is

Stage I-III Stage IV-VI Stage VII-VIII Stage IX-XI Stage XII

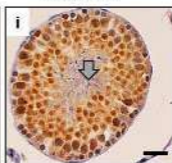
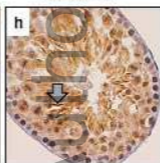
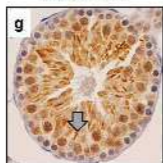


Stage IX-XI

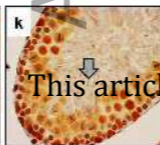
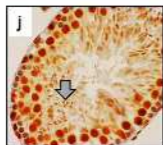
Stage XII

Stage I-III

SNAI1



LSD1



This article is protected by copyright



Minerva Access is the Institutional Repository of The University of Melbourne

Author/s:

Micati, DJ; Hime, GR; McLaughlin, EA; Abud, HE; Loveland, KL

Title:

Differential expression profiles of conserved Snail transcription factors in the mouse testis

Date:

2018-03-01

Citation:

Micati, D. J., Hime, G. R., McLaughlin, E. A., Abud, H. E. & Loveland, K. L. (2018).
Differential expression profiles of conserved Snail transcription factors in the mouse testis.
ANDROLOGY, 6 (2), pp.362-373. <https://doi.org/10.1111/andr.12465>.

Persistent Link:

<http://hdl.handle.net/11343/283540>

File Description:

Accepted version